Journal of Zhejiang University-SCIENCE A (Applied Physics & Engineering)
ISSN 1673-565X (Print); ISSN 1862-1775 (Online)
www.zju.edu.cn/jzus; www.springerlink.com
E-mail: jzus@zju.edu.cn

Behavior of reinforced concrete structural walls with various opening locations: experiments and macro model*

Ji-yang WANG†1, Masanobu SAKASHITA[2], Susumu KONO[2], Hitoshi TANAKA[3], Wen-juan LOU[1]

([1]*Institute of Structural Engineering, Zhejiang University, Hangzhou 310058, China*)

([2]*Department of Architecture, Kyoto University, Kyoto 615-8012, Japan*)

([3]*Disaster Prevention Research Institute, Kyoto University, Kyoto 611-0011, Japan*)

†E-mail: jiyang.wang@gmail.com

Received July 4, 2009; Revision accepted Sept. 30, 2009; Crosschecked Jan. 18, 2010

Abstract: Two experimental tests of three-storied reinforced concrete structural walls having large openings were performed. Based on an original macro model, a multiple modified macro-model was proposed to develop a simple method to design a reinforced concrete structural wall with large openings and various opening locations. The interaction between reinforcement ties and concrete struts formed along the perimeter of openings was neglected in the original model. However, the strut-and-tie node was proposed to take account of such interaction in the proposed model. The predicted behavior of two specimens using such a proposed model was compared with the experimental results. It is shown that the behavior of structural walls with large openings could be modeled well using the proposed model. Moreover, the study indicates that the proposed model is applicable even in cases of multi-story structural walls having large openings and various opening locations.

Key words: Structural wall, Shear behavior, Multiple modified macro model, Various opening locations, Opening ratio
doi:10.1631/jzus.A0900400 **Document code:** A **CLC number:** TU375

1 Introduction

Structural walls have been usually adopted as the main earthquake-resistant components of reinforced concrete buildings. However, they usually have some openings according to the intention of the architectural design, and the opening ratios, locations and shapes are often various. Therefore, some corresponding structural details and restrictions have been provided in both national and international seismic design codes. In the current design code of Architectural Institute of Japan (AIJ, 1999), the minimum strength reduction factor of a structural wall due to the openings is limited to 0.6 by restricting the maximum ratio of opening dimensions to the corresponding wall length and height. And in the seismic code of China (GB50011-2001, 2008), the opening area is generally limited to less than 15% of the area of wall. These limits and restrictions are provided to make the conventional method applicable to wall structures, where the method is based on the past experimental data and observation. If the opening dimensions do not satisfy the above restrictions, one is required to solve the structure as a frame having a finite rigid area for the beam column joint. If the opening locations are too eccentric and/or the shapes of large openings are not rectangular, the strain distribution is significantly non-linear and the finite element method (FEM) analyses are often used. During the past two decades, much work on FEM analyses of structural walls has been undertaken (Inoue *et al*., 1998; Fujita *et al*., 2001; Palermo and Vecchio, 2007), but it always takes more time for the design. From the above point of view, it is desirable to develop a simple but rational method. Schlaich and Schäfer (1991) proposed a strut-and-tie

* Project supported by the Grants-in-Aid for Scientific Research of Japan (No. 16206056), and the Scientific Research Foundation for Talent Introduction (No. 113201-811132), Zhejiang University, China

model to design the strain distribution region which covered also the details consistently for all types of concrete structure, just like a beam-column joint or deep beam. And applications of such a strut-and-tie model to reinforced concrete structures with/without openings have been treated extensively (Hwang *et al*., 2001; Tjhin and Kuchma, 2002; Tan *et al*., 2003), but there are only a few examples for reinforced concrete structural walls (Paulay and Priestley, 1992). In addition, much research on modeling a shear wall without openings has been done to represent the flexural behavior and the shear behavior (Ghobarah and Youssef, 1999; Orakcal *et al*., 2004; Orakcal and Wallance, 2006; Jalali and Dashti, 2008), but the influence of a frame column or beam was not taken into account. Takehara and Motitsuki (1993), proposed a macro model of a single-story structural wall with opening to evaluate the strength and deformation based on a strut-and-tie model. Though good results were found, the applied examples were only a few, and also no method for applying these to the cases of continuous walls above the height of a multi-story building was exhibited. Moreover, the interaction between wall reinforcement ties and concrete struts formed possibly along the perimeter of openings was neglected in their model. The neglect of such interaction will result in an underestimate of strength capacity and stiffness of walls if the openings are comparatively large.

In this study, a multiple modified macro model, which takes account of the possible interaction mentioned above, was proposed by modifying the original macro model of Takehara and Motitsuki (1993). The adequacy of the proposed model was testified by carrying out seismic loading tests on two of the 40% scale specimens of reinforced concrete structural walls having the same opening ratio and various opening locations. Moreover, the behavior predicted using the proposed model was compared with that of the experimental tests.

2 Experimental

2.1 Specimens

As analytical objects of this study, two specimens named as L1 and L3 were used (Fig. 1). They were 40% scale models of concrete structural walls with eccentric openings (L1) or central openings (L3), and the experimental tests were conducted at Kyoto University, Japan (Warashina *et al*., 2007; 2008).

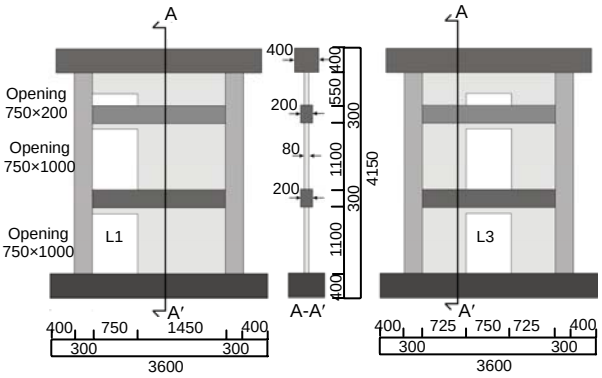

Fig. 1 Dimension of specimens (mm)

The height and the span length of the specimen can be seen in Fig. 1. The sectional dimensions also some details of beams, columns and wall are listed in Tables 1 and 2, respectively. D and Φ present the different types of reinforcements, respectively. Material properties of reinforcement and concrete adopted for the specimens are listed in Tables 3 and 4, respectively. The opening ratio adopted as an experimental parameter is 0.46 for two specimens, where it is defined as $(h_0 l_0/hl)^{1/2}$, where l_0 and h_0 are the length and height of the opening, respectively, l is the center to center spacing between two side columns, h is the center to center spacing between the upper and lower beams. The opening location of L1 is eccentric, while L3 is central.

Table 1 Section and reinforcements of beam/column (mm)

	Section dimension	Main reinforcement	Hoop reinforcement
Side column*	300×300	8-D19	2-Φ10@75
Beam	200×300	2-D13	2-Φ6@100
Foundation beam	600×400	4-D25	4-D10@100
Loading beam	400×400	2-D25	2-D10@100

* For example, the side column section contains eight D19 bars, with Φ10 double closed stirrups spaced at 75 mm

Table 2 Section and reinforcements of wall (mm)

	L1	L3
Thickness (mm)	80	80
Wall reinforcement	D6@100	D6@100
Reinforcing bar of opening (V)	1-D16	4-D13
Reinforcing bar of opening (H)	2-D13	4-D10

V: vertical; H: horizontal

Table 3 Properties of reinforcements (mm)

	Yield strength (MPa)	Ultimate strength (MPa)	Young's modulus (GPa)
D6	425	538	204
D10	366	509	180
D13	369	522	189
D16	400	569	194
D19	384	616	183

Table 4 Properties of concrete

	Compressive strength (MPa)	Tensile strength (MPa)	Young's modules (GPa)
L1	28.9	2.2	26.0
L3	32.7	2.9	23.3

As one of the aims of this study was to clarify the effect of openings on the shear behavior of a structural wall, both specimens were designed to fail in shear, not in flexure.

Noted that the maximum opening ratio is limited to 0.4 in the design code of AIJ (1999) when the wall strength reduction factor due to opening is determined by the empirical equations specified in the code.

2.2 Loading system

Fig. 2 shows the loading system and the specimen L1. The lateral load Q was applied statically to the loading beam through the arm and the steel plates by two 2000-kN hydraulic jacks. Cyclic reversed horizontal loads were statically applied to the specimens in both positive and negative directions, simulating earthquake forces. Loading was mainly controlled by measured displacement in terms of the story drift angle. The first cycle of loading was performed up to 200 kN, subsequently two cycles of repeated loading were applied for each drift angle up to ±0.04%, ±0.1%, ±0.25%, ±0.5%, ±0.75% and ±1.0%.

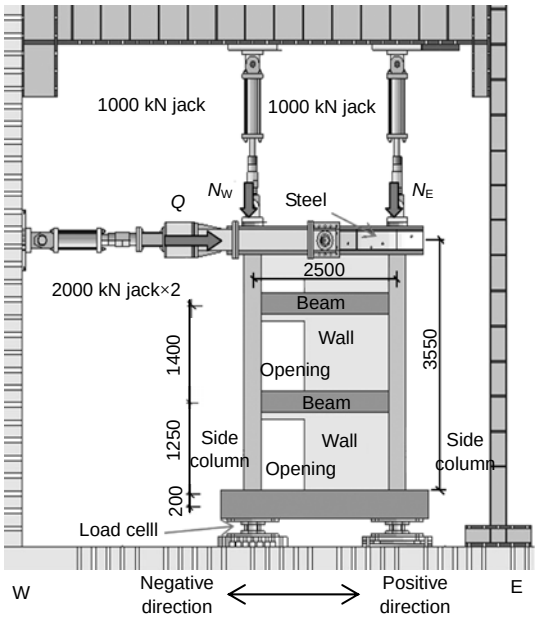

Fig. 2 Loading system

N_W and N_E are axial forces from west and east, respectively

During the cyclic horizontal loading, vertical axial loads were also applied by two 1000-kN hydraulic jacks assuming that the specimens are representing a part of the lower three stories of a typical reinforced concrete building with six stories. Hence, the vertical axial load was determined in accordance with the assumed long-term axial loads for a six-storied wall with one span. Thus, 488 kN (244 kN for each jack) was determined as the basic axial load. Moreover, controlling two hydraulic jacks, two vertical axial loads were adjusted to each other so as to keep the apparent shear span ratio ($M/(Qd)$) always 1.0, where M is the flexural moment applied to the base of the wall, Q presents the horizontal load applied to the loading beam, and d is the distance between the center to center spacing between two side columns. This is to make the shear damage in the wall precede the flexural yielding of the wall. However, the effect of the axial load on the shear behavior of each wall was insignificant as far as these test results were concerned, because the side columns were not damaged till the end of the tests.

2.3 Test results

Fig. 3 and Fig. 4 show the damage observed in two specimens at 0.75% drift and at the end of the tests, respectively.

In both specimens, the shear cracks in the wall and the flexural cracks in the tensile side column were observed before a drift angle of 0.05%, and the cracks increased until a drift angle of 0.5%. When the drift angle increased from 0.5% to 0.75%, the load reached the maximum and the damage to the walls and the crack in the upper part of the openings progressed for further loading after the maximum load. Moreover, some parts of the main longitudinal bars of the beam and the reinforcements of the wall were revealed due to spalling of cover concrete, and the buckling of the wall reinforcements in the first story were observed.

In the L1 specimen, the shear cracks in the wall of the first story and the flexural cracks in the tensile

column of the first story were observed at a drift angle of +0.04%. At a drift angle of +0.25%, the cracks in the upper part of the opening (part A in Fig. 3a) progressed along the opening reinforcement. And the cracks were not formed much in the short span beam of the second and third stories. At a drift angle of −1.0%, shear sliding occurred in the wall of the first story (part C in Fig.3b), the lateral reinforcing bars of the wall were bent seriously and the cracks have been propagated greatly along the wall reinforcement. At a drift angle of +1.5%, the strength was decreased suddenly for the shear damage in the wall of the second story (part D in Fig. 3b).

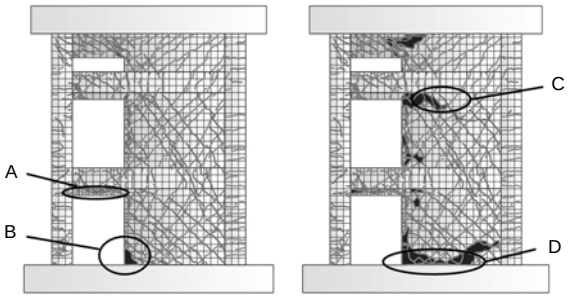

Fig. 3 Observed damage of L1 at (a) 0.75% drift and (b) end of the tests

The solid lines show the cracks and the painted parts show the severely damaged area

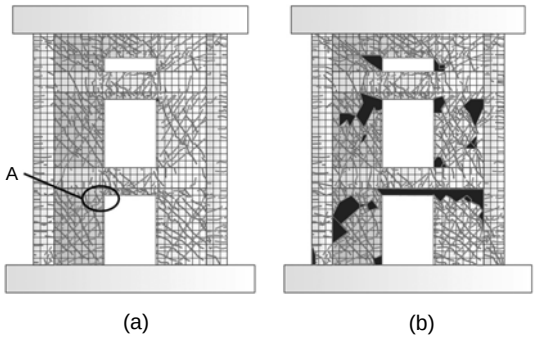

Fig. 4 Observed damage of L3 at (a) 0.75% drift and (b) end of the tests

The solid lines show the cracks and the painted parts show the severely damaged area

In the L3 specimen, the cracks in the wall of the first story and in the upper comer of the opening (part A in Fig. 4a) were observed at a drift angle of 0.05% and then the stiffness was decreased. Since a drift angle of 1.0%, the strength was gradually decreased without shear sliding observed in the wall of the first story. Moreover, damage to the boundary beam between a couple of walls was negligible till the end of the loading. For the central opening location and the difficulties of composing the compressive strut over two stories, the shear cracks over two stories were only a few.

Concerning the yield point of the wall reinforcements, most of the lateral reinforcements of two specimens yielded at a drift angle of 0.5%, while most of the vertical reinforcements yielded at a drift angle of 1.0%. However, at a drift angle of −0.5%, the vertical wall reinforcements near the opening (part B in Fig. 3a) were buckled in compression. In case of negative direction loading, the above results indicate that the compressive stress will be concentrated at the opening corner.

Fig. 9 (in subsection 4.2) shows the relationships between the lateral load and the drift angle. It can be seen that the maximum lateral strength of L1 is lower than that of L3 because the opening location of L1 is eccentric. It can be also found in both test specimens that the strengths attained during the positive direction loading are larger than those during negative direction loading. The strength degradation after the peak load can be seen more or less in both specimens. However, strength degradation is not sudden in L3.

With respect to the failure mode, L1 failed in a comparatively ductile manner after flexural yielding of the short span beams and reached the final stage due to the shear slip damage of the wall.

3 Multiple macro model

As shown in Fig. 5, the original macro model proposed by Takehara and Motitsuki (1993) corresponds to a situation where diagonal cracks have been formed and significantly developed in the wall. In this model, it was assumed that each of the objective walls can be treated as a single-story wall which was taken out from the whole wall structure, and the beams were treated as rigid elements without axial springs and shear springs.

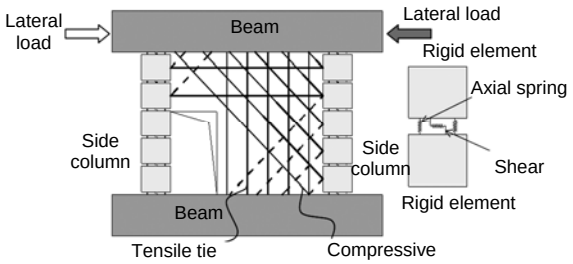

Fig. 5 Original macro model (Tokehara and Motitsuki, 1993)

3.1 Multiple original macro model (O-M model)

In this study, a multiple original macro model (O-M model) shown in Fig. 6 was assembled based on the original macro model. N_1 and N_2 present the axial load applied to two side columns, respectively.

It is composed of an upper and a lower beam (that is, loading beam and foundation beam), the side columns, the compressive concrete struts and the tensile reinforcement ties of the wall. The angle of the inclined compressive struts is assumed to be a constant degree against the horizontal axis. The compressive struts and the vertical/horizontal tensile ties which are placed in the direction passing through the openings are assumed to be ineffective and hence neglected. The loading beam and the foundation beam are treated as a rigid element. The side columns and beams are represented by a model composed of the rigid elements, the elasto-plastic axial springs and the shear springs. The height of the beam and the width of column could be taken as the dimensions of these rigid elements, respectively. The struts and the ties could be connected to corresponding rigid elements with an inclination of 45°. The axial springs are placed at the center of the main reinforcement of one side.

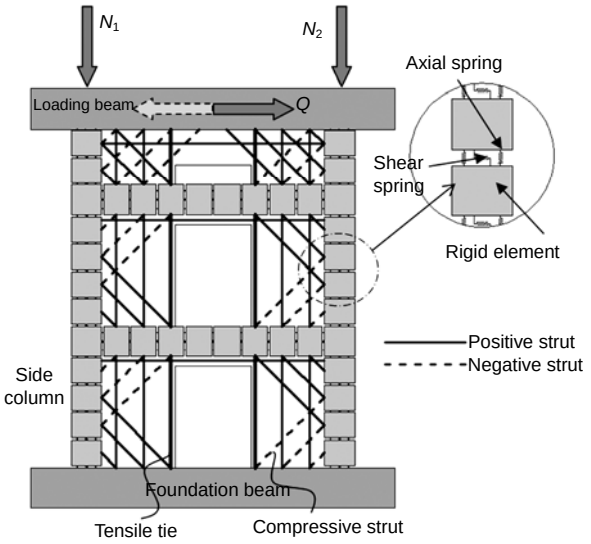

Fig. 6 Multiple original macro model (L3)

The strength and the rigidity of the axial spring and the rigidity of the shear springs are expressed as follows:

Axial strength of the spring in tension:

$$ {}_{c}N_{nt}=A_g\times {}_{g}\sigma_y/2, \tag{1}$$

where A_g is the main bar area of side column and ${}_{g}\sigma_y$ is the yield strength of side column main bar.

Axial rigidity of the spring in tension:

$$ {}_{c}K_{nt}=E_sA_g/(2\Delta h), \tag{2}$$

where E_s is the reinforcement Young's modulus and Δh is the distance between two rigidities.

Axial strength of the spring in compression:

$$ {}_{c}N_{nt}=(A_g\times {}_{g}\sigma_y+bD\sigma_d)/2, \tag{3}$$

where bD is a section area of side column and σ_d is the concrete compressive strength.

Axial rigidity of the spring in compression:

$$ {}_{c}K_{nc}=(E_sA_g+E_cbD)/(2\Delta h), \tag{4}$$

where E_c is the concrete Young's modulus.

Rigidity of the shear spring:

$$ {}_{c}K_{s}=({}_{c}K_n/{}_{c}K_{nc})\times(GbD/\Delta h), \tag{5}$$

where ${}_{c}K_n$ is an average of the rigidity of two axial springs at the same loading cycle which is determined taking account of the progress of the horizontal cracks in the column, and G is the concrete shear modulus. Hence, the term of ${}_{c}K_n/{}_{c}K_{nc}$ in Eq. (5) expresses the reduction in the shear rigidity due to such cracks.

The model ties are substituted for the vertical/horizontal reinforcements placed within the strip element with width b_w, and their strength and rigidity are expressed as follows:

Tie strength:

$$ {}_{b}N_t=\rho_s\times {}_{s}\sigma_y b_w t, \tag{6}$$

where ρ_s is a reinforcement ratio of wall, ${}_{s}\sigma_y$ is the yield strength of wall reinforcing bars, b_w is the width of a strut, and t is the thickness of a wall.

Tie rigidity:

$$ {}_{b}K_n=\rho_sE_sb_wt/L, \tag{7}$$

where L is the length of a wall.

The compressive concrete struts follow the concrete constitutive law of Popovics (1971) below:

$$\sigma = n\xi/(n-1+\xi^n)\times\sigma'_B, \quad (8)$$

where $\sigma'_B=0.63\sigma_B$, $n=0.57\times10^{-2}\sigma'_B/9.8+1$, $\xi=\varepsilon/\varepsilon_0$, $\varepsilon_0=4.29\times10^{-4}(\sigma'_B)^{0.25}$. The first term, σ'_B, is the effective concrete compression strength of the wall where the parallel shear cracks are ideally formed and developed and the coefficient 0.63 was proposed from the experiment without openings by Takehara and Motitsuki (1993). ε and ε_0 is the strain of concrete and the strain corresponding to the concrete maximum compression stress, respectively.

3.2 Multiple modified macro model (M-M model)

Fig. 7 shows the multiple modified macro model (M-M model) which was assembled by modifying the original model. In this model, the effect of the tensile ties placed around the openings is taken into account. The main modified items are as follows:

1. As shown in Figs. 6 and 7, the beams were modeled using the rigid elements, the elasto-plastic axial springs and the shear springs like the side column. The compressive struts and the tensile ties in two adjacent story walls were connected by the beam rigid elements.

2. The O-M model did not take account of the effect of the reinforcements around the openings. However, the M-M model considered the effect of the vertical reinforcements around openings, on the premise that they were sufficiently anchored in the upper and lower beams. Moreover, it also considered the effect of the horizontal reinforcements around the openings, on the premise that they were anchored to the side columns and/or the vertical reinforcement placed near the perimeter of the opening. Therefore, the vertical and horizontal reinforcements around the opening were modeled as the ties and they were connected to the struts which were assumed to be formed in the direction passing through the opening. In this model, the force as the resultant of stress transferred from the struts can be equilibrated with that of the stress in ties at the CTT node (ACI Committee 318, 2008).

3. Popovic (1971)'s concrete constitutive law was used to solve the O-M model, while the Vecchio-Collins concrete constitutive law (Vecchio and Collins, 1986) was used instead in the M-M model. The concrete tensile stress has not been considered in both macro models.

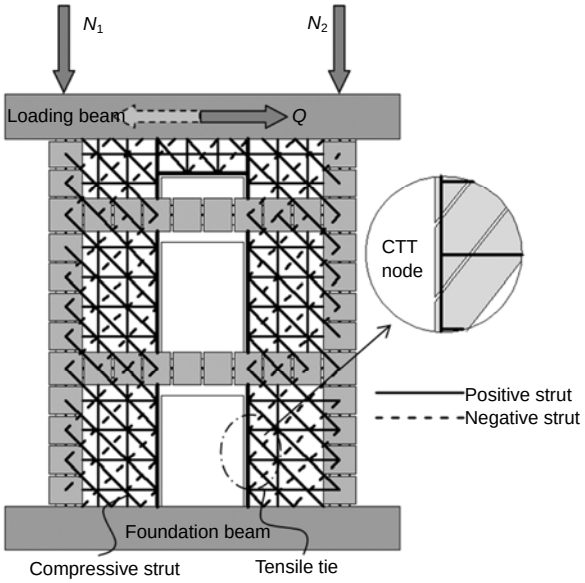

Fig. 7 Multiple modified macro model (L3)

4 Analysis

4.1 Analysis detail

The side columns of two models were divided into 5 segments, and the compressive struts were arranged in the form of strip elements with a width of about 25 cm. The material constants were determined according to the measured mechanical properties of materials. The mechanical properties of axial spring, the shear spring and the reinforcement tie were determined in accordance with the original macro model by Takehara and Motitsuki (1993). However, the concrete constitutive law based on the Vecchio-Collins (1986)'s model was modified as follows:

Ascending branch: $\varepsilon_d \le \varepsilon_0/\lambda$,

$$\sigma_d = f_c\left[2\left(\frac{\varepsilon_d}{\varepsilon_0}\right)-\lambda\left(\frac{\varepsilon_d}{\varepsilon_0}\right)^2\right]. \quad (9)$$

Descending branch: $\varepsilon_d > \varepsilon_0/\lambda$,

$$\sigma_d = \frac{f_c}{\lambda}\left[1-\left(\frac{\varepsilon_d/\varepsilon_0-1/\lambda}{2-1/\lambda}\right)^2\right], \quad (10)$$

where ε_0 is the strain corresponding to the concrete maximum compression stress and is assumed to be

0.002. λ is a constant (Belarbi and Hsu, 1994) when applied to a wall without opening and can be expressed as

$$\lambda=1/\cos\alpha, \tag{11}$$

where the angle α was assumed to be 45° based on the observed damage of the specimens.

As shown in Fig. 8, three concrete constitutive laws were used in macro model analyses for this study.

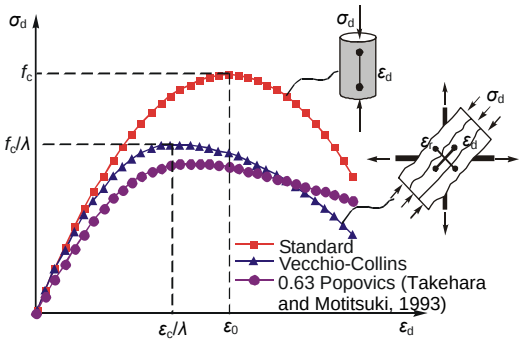

Fig. 8 Concrete constitutive law

The stress-strain relationship of reinforcement was expressed by a bi-linear model where the tangential stiffness in the post-yield stage was assumed to be 1% of the initial stiffness. However, the compression stress induced in the reinforcement was neglected. As the boundary condition, each side central node connected to the load cells was treated as a pin support.

The push-over analyses were conducted with a horizontal displacement increment of D=0.5 mm. As the first step, the long term axial loads of 244 kN were applied to each of the side columns. For further loading, these axial loads were varied with ±0.42 kN in two specimens, per 1 kN of the horizontal load change in accordance with the increase in lateral displacement. The horizontal force was applied to the center of the loading beam in the same manner as the actual testing.

4.2 Analysis results

The relationships of lateral load vs. drift angle for L1 and L3 are shown in Fig. 9. Table 5 and Table 6 show the comparison of maximum strengths and initial stiffness between the results of each model and the experimental test, respectively.

The envelope curves of lateral load-drift angle relationships obtained from the M-M model agree well with those of the experimental results in both positive and negative loadings of two specimens (Fig. 9). In the cases of L1 and L3, the tensile ties above the opening of the first and the second stories yielded at drift angles of about 0.5% and 0.4%, respectively. But other horizontal ties did not yield for shear redistribution unlike the experimental results. As shown in Fig. 10, the compressive struts connected to the foundation beam of the first story yielded at drift angles of ±0.6% and ±0.5%, respectively. The load carrying capacity started to decrease after the struts had yielded. However, any sudden decrease or crushing of the struts was not observed because of the shear redistribution and the assumption of the concrete constitutive law. Moreover, the M-M model predicted well the behavior in the post-peak regions, although the computed value is a little bit bigger than the experimental value. This is because the strength deterioration of concrete struts was comparatively prompt due to the cyclic reversed loading in the actual test specimens, while the analyses were conducted in the manner of a one way push-over.

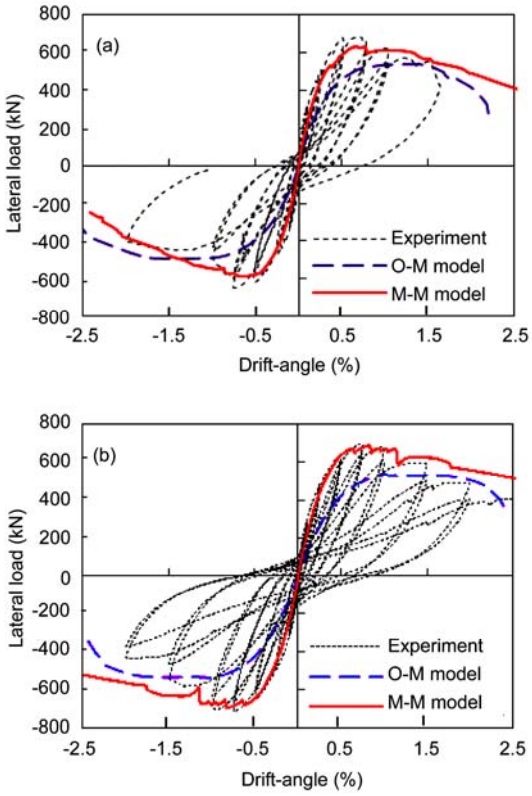

Fig. 9 Lateral load-drift angle for (a) L1 and (b) L3

Table 5 Comparison of ultimate strength between experiment, O-M model, and M-M model (kN)

	L1		L3	
	Positive	Negative	Positive	Negative
Experiment	686	−649	701	713
O-M model	540 (0.79)	−496 (0.76)	536 (0.79)	−536 (0.75)
M-M model	632 (0.92)	−589 (0.91)	691 (0.99)	−691 (0.97)

Note: the value in parenthesis is the ratio of the analytical results to experimental value

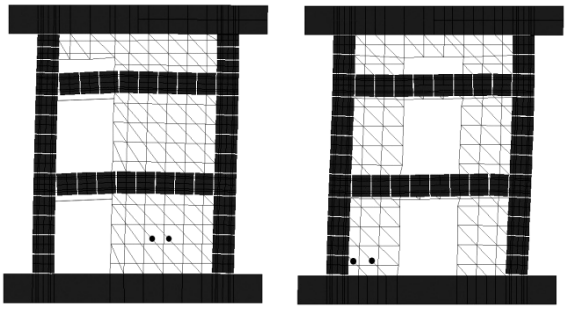

(a) (b)

Fig. 10 Deformation and damage of M-M models for (a) L1 and (b) L3

• represents struts reached the maximum strength

The computed ultimate strengths of the O-M model are much smaller than experimental values, while the ratios between strengths of the M-M model and that of experimental value show a high degree of precision in both positive loading and negative loading (Table 5). However, the stress of the axial spring in the side columns did not reach the yield strength.

As listed in Table 6, the initial stiffness of the O-M model is much smaller than the experimental results, because the macro model corresponds to a situation where the diagonal cracks have been formed and significantly developed, and the dowel action of reinforcement and the aggregate action of concrete was neglected. However, the initial stiffness of the M-M model is much closer to the experimental values.

Table 6 Initial stiffness between experiment, O-M model, and M-M model

	L1		L3	
	Positive	Negative	Positive	Negative
Experiment	6.17	6.72	4.50	4.52
O-M model	2.60 (0.42)	2.05 (0.31)	1.87 (0.42)	1.87 (0.41)
M-M model	4.17 (0.68)	4.26 (0.63)	3.72 (0.83)	3.72 (0.82)

Note: the value in parenthesis is the ratio of the analytical results to experimental value

These model results corresponded well with the experimental observation, except for the behavior after the shear sliding of the walls.

4.3 Shear distribution

The shear of wall and columns was not directly observed in the experimental tests, while the analyses can take out the shear of each component by a simple method. Figs. 11 and 12 show the shear distribution between the top/bottom section of the first story wall and that of two side columns. The total shear of the top/bottom section of the first story wall and side columns used here was taken to be the same value of the lateral load.

The shear of the first story wall gradually decreased while the drift-angle increased in two specimens, and that of the side columns has an opposite tendency.

As shown in Fig. 11a, the shear carried by the bottom section of wall was only about 20% of total shear, yet that of the top section of the wall was about 80% in the post-yield stage. Because the large openings interrupted the shear transfer path to the foundation beam, the main part of the shear transferred directly from the beam to the side column through the diagonal struts. The tensile ties around the openings are effective in the shear transfer, but limited.

As shown in Fig. 11b, for the lateral load applied from the side having no openings, the main part of the shear was transferred to the foundation beam through diagonal struts for the definite shear transfer path. In the post-yield stage, the shear carried by the bottom section of wall and columns was about 50%.

As shown in Fig. 12, in the post-yield stage, the main part of shear was carried by the wall. The bottom section of wall carried 50%–60% of shear stress before reaching the maximum lateral load, while the top section of wall carried 80% of shear or more. Since the drift angle of 0.4% for the main concrete struts yielded, the shear carried by the wall starts decreasing. After reaching the maximum lateral load, the shear stress carried by the bottom section of wall was less than 50% and that of the columns started increasing. At the end of the test, 30%–40% of shear was still carried by the bottom section of wall for the ductility, and the top section carried about 60% of shear.

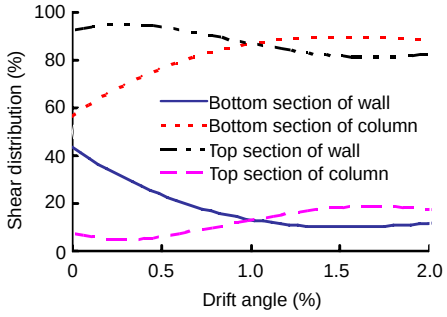

(a)

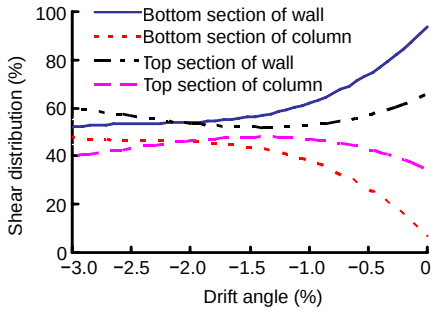

(b)

Fig. 11 Shear distribution (L1). (a) Positive loading; (b) Negative loading

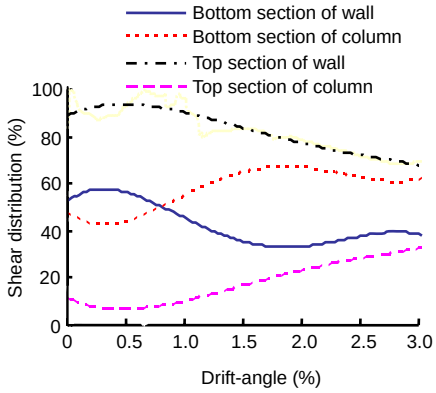

Fig. 12 Shear distribution (L3)

From mentioned above, in such cases having large openings, close relationships between the opening location or the loading direction and the shear carried by the wall are revealed. If the loading direction is negative, whatever the opening location, the main part of shear is carried by the bottom section of the first story wall. If the loading direction is positive, the main part of shear is carried by the bottom section of first story columns and there is little contribution from some parts of the wall in loading transfer. This behavior is worth studying for the seismic design of multi-story structural walls with large openings.

5 Discussions and conclusions

In this study, two experimental tests of three-storied structural walls with openings were performed, and an M-M model was proposed by modifying an original macro model to obtain more accurate load-deformation relationships and behaviors in the case of multi-story walls with various large opening locations. The main discussions and conclusions are summarized as follows:

1. Behaviors of a structural wall with eccentric openings become different depending on the loading direction, and the ultimate strength becomes different depending on the opening locations. However, the opening locations and/or loading direction are not taken into account in the current design code. The calculation formula of lateral strength capacity using the opening ratio in the current design code needs to be improved, based on the shear resistance mechanism and the extensive experimental studies.

2. Although the specimens were designed according to the current design code, the shear slip failure in the first story wall with eccentric openings still occurred at the final stage. This result suggests that the details of the seismic design code in such a region need to be improved.

3. It is confirmed by the comparison between the analytical results and the experimental results that the M-M model could predict the different behaviors of the structural walls with various opening locations and different loading directions well, and the M-M model is applicable to structural walls even in the case of the opening ratio exceeding 0.4.

4. Comparison of strength, stiffness, lateral load-drift angle relationship between M-M model and the O-M model indicates that the M-M model is more adequate.

Some extensive studies are expected for the application of the efficient method proposed in this study to account for the shear behavior of structural walls with various opening ratios.

Acknowledgement

The authors appreciate the great assistance of graduate students M. WARASHINA, K. MORI, and K. CHOSA, Kyoto University, Japan, in the execution of experiments and the data process.

References

ACI Committee 318, 2008. ACI 318-08/318R-08, Building Code Requirements for Structural Concrete and Commentary. American Concrete Institute, Appendix A, p.378-394.

AIJ, 1999. AIJ Standard for structural calculation of reinforced concrete structures based on allowable stress concept. Architecture Institute of Japan Press, Tokyo, Japan.

Belarbi, H., Hsu, T.C.C., 1994. Constitutive laws of concrete in tension and reinforcing bars stiffened by concrete. *ACI Structural Journal*, **91**(4):465-474.

Fujita, T., Shirai, N., Watanabe, K., 2001. Seismic response analysis of RC shear walls by nonlinear FEM. *Transaction of the Japan Concrete Institute*, **23**:223-230.

GB50011-2001, 2008. Code for Seismic Design of Building. Architecture & Building Press, Beijing, China.

Ghobarah, A., Youssef, M., 1999. Modeling of reinforced concrete structural walls. *Engineering Structures*, **21**(10):912-923. [doi:10.1016/S0141-0296(98)00044-3]

Hwang, S.J., Fang, W.H., Lee, H.J., Yu, H.W., 2001. Analytical model for predicting shear strength of squat walls. *Journal of Structural Engineering, ASCE*, **127**(1):43-50. [doi:10.1061/(ASCE)0733-9445(2001)127:1(43)]

Inoue, N., Yang, K.J., Shibata, A., 1998. Dynamic nonlinear analysis of reinforced concrete shear wall by finite element method with explicit analytical procedure. *Earthquake Engineering & Structural Dynamics*, **26**(9): 967-986. [doi:10.1002/(SICI)1096-9845(199709)26:9<967::AID-EQE689>3.0.CO;2-T]

Jalali, A., Dashti, F., 2008. Nonlinear Behavior of Reinforced Concrete Shear Walls Using Macro Model. AIP Conference Proceedings of Seismic Engineering Conference: Commemorating the 1908 Messina and Reggio Calabria Earthquake, **1020**:979-986. [doi:10.1063/1.2963940]

Orakcal, K., Wallance, J.W., 2006. Flexural modeling of reinforced concrete walls-experimental verification. *ACI Structural Journal*, **103**(2):196-206.

Orakcal, K., Wallance, J.W., Conte, J.P., 2004. Flexural modeling of reinforced concrete walls-model attributes. *ACI Structural Journal*, **101**(5):688-698.

Palermo, D., Vecchio, F.J., 2007. Simulation of cyclically loaded concrete structures based on the finite-element method. *Journal of Structural Engineering*, **133**(5):728-738. [doi:10.1061/(ASCE)0733-9445(2007)133:5(728)]

Paulay, T., Priestley, M.J.N., 1992. Seismic Design of Reinforced Concrete and Masonry Buildings. John Wiley and Sons, New York, p.486-488. [doi:10.1002/9780470172841]

Popovics, S., 1971. Factors Affecting the Elastic Deformation of Concrete. Proceedings of the International Conference on Materials, Kyoto, **IV**:172.

Schlaich, J., Schäfer, K., 1991. Design and detailing of structural concrete using strut-and-tie models. *The Structural Engineer*, **69**(6):113-125.

Takehara, M., Motitsuki, M., 1993. Elasto-plastic Analysis of Framed Shear Walls with an Opening Using Macro Model. Summaries of Technical Papers of Annual Meeting Architectural Institute of Japan, **Structures IV**:303-304 (in Japanese).

Tan, K.H., Tong, K., Tang, C.Y., 2003. Consistent strut-and-tie modeling of deep beams with web openings. *Magazine of Concrete Research*, **55**(1):65-75. [doi:10.1680/macr.55.1.65.37555]

Tjhin, T.N., Kuchma, D.A., 2002. Computer-based tools for design by the strut-and-tie method: advances and challenges. *ACI Structural Journal*, **99**(5):586-594.

Vecchio, F.J., Collins, M.P., 1986. The modified compression field theory for reinforced concrete elements subjected to shear. *ACI Structural Journal*, **83**(2):219-231.

Warashina, M., Mori, K., Wang, J.Y., Sakashita, M., Kono, S., 2007. Shear Behavior of Multi-story Shearwalls with Eccentric Openings. Summaries of Technical Papers of Annual Meeting Architectural Institute of Japan, **Structures IV**:677-682 (in Japanese).

Warashina, M., Kono, S., Sakashita, M., Tanaka, H., 2008. Shear Behavior of Multi-story RC Structural Walls with Eccentric Openings. The 14th World Conference on Earthquake Engineering, Beijing, China, **S15**-029.